104 (2025) 104583

Contents lists available at ScienceDirect

Poultry Science

journal homepage: www.elsevier.com/locate/psj

miR-1458 is inhibited by low concentrations of Vitamin B6 and targets TBX6 to promote the formation of spermatogonial stem cells in Rugao Yellow Chicken

Qingqing Geng [a,b], Cai Hu [a], Ziduo Zhao [a], Zhe Wang [a], Fufu Cheng [a], Jing Chen [a], Qisheng Zuo [a], Yani Zhang [a,*]

[a] Key Laboratory of Animal Breeding Reproduction and Molecular Design for Jiangsu Province, College of Animal Science and Technology, Yangzhou University, Yangzhou, PR China
[b] College of Veterinary Medicine, Yangzhou University, Yangzhou, PR China

ARTICLE INFO

Keywords:
Rugao Yellow Chicken
Spermatogonial stem cell
miR-1458
TBX6

ABSTRACT

Spermatogonial stem cells (**SSCs**) have vast application prospects in livestock and poultry production, genetic engineering, and medical research. However, the scarcity of SSCs and the complexity of their development limit the elucidation and verification of the mechanism of SSCs in vitro. Although miRNAs have been identified as critical players in germ cell development, upstream regulatory mechanisms by which miRNAs regulate SSCs formation are rarely reported. In this study, miR-1458, which was differentially expressed during SSCs formation, was selected by transcriptomic sequencing. We found that miR-1458, inhibited in an in vitro SSCs induction model,

significantly upregulated the expression of germline marker genes (*Cvh* and *integrin β1*). Further analysis using Immunofluorescence and Flow Cytometry confirmed that miR-1458 inhibition promotes the formation of spermatogonial stem-like cells (**SSCLCs**). Immunohistochemical significantly increased the number of SSCs in the testis in vivo. However, significant upregulation of miR-1458 showed opposite results. High-throughput sequencing results showed that miR-1458 interacted with *TBX6*, one of the target genes of miR-1458, involved in affecting cell differentiation, and dual-luciferase reporter vectors confirmed the targeting relationship between the two. *TBX6* overexpression and knockdown in vitro and in vivo have validated its function in SSCs formation. We found that overexpression of *TBX6* promoted SSCs formation. Additionally, we identified Vitamin B6, a key metabolite affecting SSCs formation, as an upstream regulator of miR-1458 expression. The results showed that low concentrations of Vitamin B6 led to low expression of miR-1458 by decreasing histone demethylation levels. Overall, our findings suggest that miR-1458 is involved in SSCs formation, which is inhibited by low concentrations of Vitamin B6 and subsequently regulates the formation of SSCs by targeting *TBX6*, an essential gene involved in embryonic stem cell differentiation. Our study demonstrates the critical role of the Vitamin B6-miR-1458-TBX6 regulatory axis in spermatogonial stem cell formation in Rugao Yellow Chicken, providing new insights into the regulatory mechanisms by which miRNAs affect SSCs formation. It should be noted that most of the germline findings related to miRNAs were obtained by in vitro studies, and in vivo studies are needed to validate our results for clinical applications.

Introduction

Spermatogonial stem cells (SSCs) serve as the initiating cells of spermatogenesis, playing a crucial role in determining the quantity and quality of semen (Kubota and Brinster, 2018). As a result, the function of SSCs has a direct impact on the intensive production of semen. In addition to their role in determining the quantity and quality of semen, SSCs also have the unique ability to stably transmit genetic information to the next generation. This feature makes them highly valuable in a variety of applications, including germline transmission, gene editing,

Scientific section: Genetics and Molecular Biology

* Corresponding author.
E-mail address: ynzhang@yzu.edu.cn (Y. Zhang).

https://doi.org/10.1016/j.psj.2024.104583
Received 20 August 2024; Accepted 21 November 2024
Available online 25 November 2024

and regenerative medicine (Diao et al., 2022). Although SSCs are important, their complex development make it difficult to fully understand the transcriptional regulation and epigenetic basis of germ cell development. Therefore, there is a critical need to delve deeply into the molecular mechanisms underlying the formation of SSCs and overcome these limitations in order to enhance their potential applications.

Currently, research on the molecular mechanisms underlying SSCs formation primarily focuses on mammals. Previous studies have highlighted the significant role of genes such as *DDX4, DAZL, STRA8, Lin28* (Hickford et al., 2011; Chen et al., 2014; Endo et al., 2015; Boellaard et al., 2017; Wang et al., 2017; Li et al., 2019; Samsonova et al., 2021), signaling pathways such as Hedgehog-Gli1, TGF-Beta, JNK, Jak-Stat, WNT, PI3K/Akt (Xian et al., 2017; Li et al., 2017; Wang et al., 2018; Yakhkeshi et al., 2018; Clotaire et al., 2018; Young et al., 2020), and growth factors such as GDNF, PDGF (Airaksinen and Saarma, 2002; Tallquist and Kazlauskas, 2004; Parekh et al., 2019) in the formation of SSCs in mammals. Despite the significant progress made in understanding the molecular mechanisms underlying SSCs formation in mammals, it remains unclear whether these findings apply to chickens due to species differences. With the emergence of epigenetic and related regulatory mechanisms, miRNA has emerged as a powerful regulator of gene expression at the post-transcriptional level (Yang et al., 2013). Current research on miRNA regulation of SSCs primarily focuses on the downstream effects of miRNA on target genes to influence cell differentiation. For example, Zhang et al. (2021) discovered that miR-302d can inhibit the formation of chicken SSCs, while Wang et al. (2017) demonstrated that gga-miR-218 directly targets SRTA8 to inhibit spermatogenesis. However, there is still much to be done in identifying key miRNAs involved in the process of chicken SSCs formation. According to reports, Cutting et al. (2012) found that miR-1458 levels promote the development of intracellular Embryonic stem cell (**ESCs**) in chicken. However, the upstream regulators of miRNAs during SSCs development in chickens are still unknown.

Research has shown that cellular energy metabolism can regulate miRNAs and impact cell proliferation and differentiation. Specifically, cell energy metabolism can affect the expression of specific miRNAs, resulting in changes to the state of cells and even the proliferation, differentiation, and functional status of cells. This research area holds great promise (O'Shea and Paul, 2010). Furthermore, key metabolites represent an important link between intermediate metabolites and epigenetic modifications (McDonnell et al., 2016). Recent studies have begun to explore epigenetic modifications, such as histone methylation, histone phosphorylation, and histone acetylation (Tsogtbaatar et al., 2020; Zuo et al., 2020), in relation to the formation of SSCs. We, therefore, speculate that key metabolites may act as upstream regulators of miRNAs that influence SSCs formation by modulating the epigenetic landscape. Such an approach may enhance the efficiency of SSCs formation.

In this study, we aimed to screen critical miRNAs involved in developing chicken ESCs to SSCs and investigate the impact of miR-1458 on SSCs fate. Building on previous research, we explored the relationship between Vitamin B6 metabolism, the activity of key epigenetic regulators, and miR-1458 function. Our investigation focused on the mechanism by which miRNAs exert their effects, and we discovered that miR-1458 targets and regulates TBX6, a protein involved in cell development, to influence the formation of SSCs. Our results provide novel insights into the molecular mechanism underlying the link between miR-1458 and Vitamin B6 metabolism and demonstrate that low concentrations of Vitamin B6 can mediate early embryonic cell state transitions and promote germ cell development to enhance the fate determination of SSCs.

Material and methods

Ethics statement

This experimental protocol complied with the guidelines of the Academic Committee of Yangzhou University by the Administrative Measures for Experimental Animals of Jiangsu Province (Permit No. 45 of the Jiangsu Provincial Government of China) and the guidelines of the National Institutes of Health (NIH Pub. No. 85-23, revised in 1996).

Cell isolation and culture

In this experiment, the Rugao yellow chicken provided by the Poultry Research Institute of Jiangsu Province was used as the animal model, and the incubation temperature and humidity were 37.8°C and 60%, respectively. Stage X blastoderms were collected for isolation and purification of ESCs, genital ridges were isolated on day 4.5 to obtain PGCs, and testis tissues were isolated to obtain SSCs on day 18.5. The isolation and culture methods used to obtain ESCs, PGCs, and SSCs were described in previous studies (Zhang et al., 2016).

All purified ESCs were cultured in standard high-glucose DMEM medium (Gibco, USA) supplemented with 5 % fetal bovine serum (**FBS**) (Gibco, USA), 100 U/mL penicillin-streptomycin combination (Life Technologies, China), 10^{-5} mol/L Retinoic acid (**RA**) (MCE, USA), and 2 % chicken serum (Life Technologies, New Zealand) at 37°C in a 5 % CO_2 incubator (Thermo Fisher Scientific, USA).

Transcriptomic analysis

Library construction and RNA-seq sequencing of three kinds of cells

Total RNA was isolated from ESCs, PGCs, and SSCs using the Total RNA Isolation Kit (Tiangen, Shanghai, China) following the manufacturer's instructions. Each test sample utilized 3 μg of total RNA for small RNA sequencing. The RNA samples were evaluated using the Agilent 2100 Bioanalyzer (Agilent Technologies, Santa Clara, CA, USA). Adaptors were ligated to the small RNA fractions at the 5′ and 3′ ends. After amplification, the quantity and quality of the sequences (140-160 bp) in the ESCs, PGCs, and SSCs cell libraries were measured using a Qubit® 2.0 Fluorometer and Agilent 2100 Bioanalyzer (Agilent Technologies). Small RNA sequencing was performed on the NovaSeq 6000 platform at Novagene Zhiyuan Technology Co., Ltd. (Novagene, Beijing, China).

FastQC (http://www.bioinformatics.babraham.ac.uk/projects/fastqc/) was utilized to evaluate the quality of the original and trimmed sequencing libraries. The resulting data were preprocessed to remove adaptors, low-quality sequences, repeats, and small RNA sequences, including rRNA, tRNA, snoRNA, and snRNA to obtain unique sequences. These sequences were then aligned with miRNA mature sequences in miR-Base20.0 to identify conserved miRNAs between species. Furthermore, miRNA expression levels were compared among three libraries: z_4 vs. c_0, z10 vs. c_0, R_4 vs. c_0, and R10 vs. c_0. Differentially expressed miRNAs were identified in the five comparisons based on $|\text{Log (Fold Change)}| \geq 1$.

Differential expression analysis and functional enrichment

Protein interaction analysis (PPI) of TBX6 was performed using the STRING database (https://www.string-db.org/). The TBX6 node was selected to examine its "co-expression" information, and Gene Ontology (**GO**) functional annotation of TBX6 interacting proteins was conducted.

Broadly targeted metabolomics analysis

Sample preparation and extraction

The freshly fertilized eggs underwent a washing and disinfection process before isolating ESCs. SSCs were obtained by processing isolated testes until 18.5 days of hatching. During the ESCs isolation process, sexing was performed using a single panel harvested from each ESCs and

subjected to Polymerase Chain Reaction (**PCR**). The method of identifying male and female ESCs is based on the patented method, patent No. CN202010868373.6. The steps are as follows: During the process of isolating ESCs, a single blastocyst is collected and placed in a 96-well cell culture plate. After the cells were suspended in ESC factor medium, 1 μL of cell suspension was added into the PCR tube for PCR analysis. The primers used for sex determination are listed in Table 1, and the PCR reaction system and reaction protocol are detailed in Tables 2 and 3.

For the extensively targeted metabolomic analysis, three samples were collected from each group (ESCs male, ESCs female, PGCs male, PGCs female, testis, and ovary), and these samples were mixed equally, resulting in 100 individuals in each sample. These mixed samples served as quality control (**QC**) samples, with one QC sample inserted every six formal samples. The samples were transferred to glass vials with pre-chilled methanol-water (V: V = 4:1) and chloroform was added after tempering. After subjecting the samples to ice bath sonication, they were transferred to a centrifuge tube and supplemented with an internal standard (L-2-chlorophenyl alanine). Further sonication and centrifugation steps were carried out, and 1 mL of the resulting supernatant was evaporated to dryness in an LC-MS injection vial. The dried sample was re-constituted with methanol-water (V: V = 1:4), stored at -20°C for 2 hours, and centrifuged. The resulting supernatant was used for subsequent analysis.

UPLC-ESI-QTRAP-MS/MS conditions and data analysis

The analyzed samples underwent ultra-high performance liquid chromatography-electrospray ionization tandem mass spectrometry (UPLC-ESI-QTRAP-MS/MS) analysis. The UPLC column used was the Waters Acquity UPLC HSS T3 C18, and the column temperature was maintained at 40°C. The flow rate was set at 0.4 mL/min, and the injection volume was 2 μL. The solvent system used was water (0.1 % formic acid): acetonitrile (0.1 % formic acid), and the gradient program was 95:5 v/v at 0 min, 10:90 v/v at 11.0 min, 10:90 v/v at 12.0 min, 95:5 v/v at 12.1 min, and 95:5 v/v at 14.0 min. The triple quadrupole linear ion trap mass spectrometer (QTRAP) was controlled by Analyst 1.6.3 software (AB SCIEX, Framingham, MA, USA). The ESI source operating parameters were set to a source temperature of 500°C, ion spray voltages of 5500 V (positive) and −4500 V (negative), ion source gas I, gas II, and curtain gas were set at 55, 60, and 25.0 psi, respectively, and collision gas was high. The identification of metabolites was done using public databases such as HMDB, MassBank, METLIN, and MoTo DB. A specific set of multiple reaction monitoring (MRM) transitions was monitored based on metabolites eluted at each period. The resulting metabolite mass peaks were integrated by peak area, and the mass peaks of metabolites in different samples were analyzed. QC samples were prepared by mixing sample extracts to monitor the repeatability of samples analyzed under the same treatment.

For the comprehensive targeted metabolomics analysis, we compared repeated measurements between the ESCs and PGCs groups using t-tests in SPSS software (version 25.0, SPSS, Chicago, IL, USA), with a significance level set at $P < 0.05$. The data were presented as mean ± standard error (**X ± SEM**). The identified differential metabolites were annotated using the KEGG and genomic data available at http://www.kegg.jp/kegg/compound/. Pearson correlation analysis was investigated the relationship between different metabolites in distinct cell types. Principal component analysis (**PCA**) and correlation analysis were initially performed on the sequencing data, followed by differential metabolite screening using cluster analysis.

Table 1
The sequences of CHD-W primer.

Gene	*Primer sequence*
CHD-W	F:5′-CTGCGAGAACGTGGCAACAGAGT -3′ R:5′-ATTGAAATGATCCAGTGCTTG -3′

Table 2
PCR reaction systems.

Reagent	Volume
2 × Mighty Amp Buffer Ver.2	10 μL
Forward primer (F)	1 μL
Reverse primer (R)	1 μL
cDNA template	1 μL
Mighty Amp DNA Polymerase	0.4 μL
ddH_2O	To 20 μL

Table 3
PCR reaction procedures (30 cycles).

Temperature	Time
98 °C	2 min
98 °C	10 s
60 °C	15 s
68 °C	40 s

Quantitative real-time polymerase chain reaction (qRT-PCR)

Fluorescence quantitation of miRNAs

The cell or tissue samples were collected, and RNA was extracted using the miRcute miRNA extraction and isolation kit (TIANGEN, Beijing, China) (Cat. No. DP501), following the manufacturer's instructions. The cDNA was synthesized by reverse transcription using the miRcute enhanced miRNA cDNA first-strand synthesis kit (Cat. No. KR211). The reactions were prepared according to the instructions of the miRcute Enhanced miRNA Fluorescent Assay Kit (TIANGEN, Beijing, China) (Catalog No. FP411). The upstream quantitative primer sequence of miRNA-1458 was TTCCTGTGATGCTCATGAGAA, and the downstream primers were provided in the kit. The miRNA reverse transcription system is shown in Table 4. Real-time PCR assays were performed using a 7500 System fluorescence quantification instrument (Applied Biosystems, Carlsbad, California, USA). The miRNA fluorescence quantitative PCR system is shown in Table 5. The relative ex-pression was calculated using Microsoft Excel software's $2^{-\Delta\Delta Ct}$ relative quantification method.

Quantitative polymerase chain reaction (qRT-PCR)

Total RNA was extracted using the Trizol method and then reverse transcribed into cDNA, which was subsequently used as a template for qRT-PCR. The real-time PCR assay was performed using the SuperReal color fluorescence quantitative pre-mixed reagent (SYBR Green, Tiangen, fp215-02) following the manufacturer's instructions. The SYBR fluorescence reagent and 7500 System fluorescence quantitative instrument were used for the assay. Finally, the test data were analyzed using Microsoft Excel software's $2^{-\Delta\Delta Ct}$ relative quantification method. The sequences of PCR primers can be found in Tables 6 and 7. Test the efficiencies of primers by following: Select the target DNA or cDNA samples with known concentration, set up the qPCR reaction system and run the program. The samples were amplified in a qPCR instrument, and both the melting curve and the amplification curve were collected and recorded. A single, narrow, and sharp peak in the melting curve, along with an "S"-shaped amplification curve, indicate that the primers are specific and have high amplification efficiency.

Table 4
miRNA reverse transcription systems.

Reagent	Volume/quality
Total RNA	1μg-1.5 μg
2 × miRNA RT Reaction Buffer	10 μL
miRNA RT EnzymeMix	2 μL
ddH_2O	To 20 μL

Table 5
miRNA qRT-PCR systems.

Reagent	Volume
miRNA first strand cDNA	1 μL
miRcute Plus miRNA PreMix(SYBR&ROX) 10 μL	10 μL
Forward primer (F)	0.6 μL
Reverse primer (R)	0.6μL
ddH_2O	7.8 μL

Table 6
Real-time quantitative PCR primer information table.

Gene	*Primer sequence*
miR-1458	F: 5′-TTCC TGTGATGCTC ATGAGAA-3′
U6	F: 5′-GTCACTTCTGGTGGCGGTAA -3′ R: 5′-GTTCAGTAGAGGGTCAAA -3′
TBX6	F: 5′-TTTCATCAGATAGGGACG -3′ R: 5′-GGACATAGGTGCGACAA-3′
Cvh	F:5′-AGGAGGACTGGGACACG -3′ R:5′-GCCTCTTGATGCTACCG -3′
integrin β1	F:5′-TGTTTGTGGGGACCAGATTG -3′ R:5′-CCAGGTGACATTTCCCATCA -3′
β-actin	F:5′-ACCAACTGGGATGATATGGAGAA -3′ R:5′-TTGGCTTTGGGGTTCAGG -3′

Table 7
miR-1458 promoter region amplification primers.

Gene	Primer sequence
miR-1458	F:5′-atttctctatcgataggtacAGCGGGCCTGGTTCGGTG-3′ R:5′-ccaacagtaccggaatgccaGCCCTGAACGCGCCGGAC -3′

Cell transfection

miR-1458-NC, miR-1458 mimics and inhibitor purchased from Jimon Biotechnology (Shanghai) Co., Ltd. were transfected into ESCs using Fugene HD transfection re-agent (Roche, 4709705001). The transfection condition is Fugene (V): Vector (M) = 3:1. Using Fugene HD transfection reagent (Roche, 4709705001), TBX6-OE and TBX6-SH constructed and preserved in our laboratory were transfected into ESCs respectively. The transfection condition is Fugene (V): vector (M) = 3:1.

Immunofluorescence (IF)

On day 10 of the RA induction model, cells were collected and treated with different interventions. The cells were washed thrice with pre-chilled PBS and then fixed in 1 % paraformaldehyde at room temperature for 20 minutes. Next, the cells were permeabilized with 0.5% Triton X-100 (Solarbio, China, vT8200) for 15 minutes at room temperature and then blocked with 10% FBS-PBS (Gibco, USA, 10099141) for 2 hours at room temperature. The primary antibody, Integrin β1 (anti-mouse, 0.1 μg/ml, BD Biosciences, RRID: 568995), was added and incubated overnight at 4°C. Subsequently, the cells were incubated with the corresponding fluorescent secondary antibody (FITC-labeled, goat anti-mouse, 2.5 μg/ml, HUABIO, HA1003) for 2 hours at 37°C, followed by staining with 200 μL of DAPI (Beyotime, China, C1002) for 15 minutes. Finally, fluorescence was observed and captured using a fluorescence-inverted microscope (Olympus, Japan, FV1200).

Flow cytometry (FC)

Cell populations were collected on days 4 and 10 of in vitro induction under various treatment conditions. The collected cell pellets were resuspended in primary antibody dilutions of Integrin β1 (anti-mouse, 0.1 μg/ml, BD Biosciences, RRID: 568995, USA) by centrifugation at 300 g for 6 min and incubated at 37°C for two hours. Following this, the cells were again centrifuged at 300 g for 6 min, and the resulting cell pellet was washed and resuspended in PBST three times. The cell suspension was then incubated with a fluorescent secondary antibody (FITC) labeled with Goat anti-mouse (FITC-labeled, goat anti-mouse, 2.5 μg/ml, HUABIO, HA1003) for two hours at 37°C. Finally, the positive cell rate was analyzed by flow cy-tometry (BD).

Luciferase reporter assay

DF-1 cells were transfected with either miR-1458 mimics, miR-1458 inhibitor or negative control (**NC**) and additionally with pGL3-basic or Basic-miR-1458. After 48 hours, the cells were collected, 70 μL of lysis solution was added, resuspended, and lysed, and then added to 96-well microtiter plates to detect dual-luciferase activity according to the instructions of the Dual-Luciferase® Reporter Assay System kit. During the determination, 70 μL of Luciferase Substrate was added to each well, and a rapid running program in the dark read the firefly fluorescence. Then, a Stop solution was added to read the Renilla fluorescence value and complete the recording of the data. Finally, the relative fluorescence activity was calculated by dividing the firefly fluorescence value by the Renilla fluorescence value, and the experiment was repeated three times.

Assay detects vitamin B6 concentration

The concentration of Vitamin B6 in ESCs and SSCs was assessed using a Vitamin B6 assay kit (Solarbio, SV8110). A standard curve was prepared using the standard, and the cells were collected, and 0.3 mL of extract was added. The cells were then disrupted by ultrasonic waves in an ice bath set at a power of 300 W, with ultrasonic waves applied for 3 seconds and intervals of 7 seconds, for a total time of 3 min. 0.4 mL of distilled water was added, and the solution was mixed well before being centrifuged at 16,000 rpm for 10 min at 25°C. The supernatant was then collected to determine the absorbance value (ΔA). ΔA was then used to determine the corresponding X value using the standard equation Y value. The concentration of Vitamin B6 in each cell was calculated as follows: Vitamin B6 (mg/104 cell) = X × V extraction ÷ cell number (10,000) = X ÷ cell number (10,000). The experiment was repeated three times.

CCK-8 ,EdU tests and JC-1 tests

To assess the impact of Vitamin B6 on cell viability, DF-1 cells were seeded in 96-well microplates at a density of 5000 cells per well. Following treatment, CCK-8 solution (C0042, Beyotime, Nantong, China) was added to each well (10 μL CCK-8/100 μL medium) and incubated at 37°C for 2 hours. The absorbance of each well was measured using a microplate reader at a measurement wavelength of 450 nm with a reference wavelength. Cell proliferation was evaluated using an EdU kit (C0085S, Beyotime, Nantong, China), while apoptosis was assessed using the JC-1 kit (C2005, Beyotime, Nantong, China). DF-1 cells were cultured in 6-well plates at a density of 2×10^5 cells per well. The assays were conducted according to the manufacturer's instructions. The experiment was repeated three times, and the experimental group-to-control group ratio was employed for statistical comparison.

Immunohistochemical (IHC)

The testes, which had hatched at 18.5 days, were washed twice with PBS. Other tissues, such as epididymides, were removed under a microscope. The testes were then fixed in Bouin's fixative for 24 hours and sent to Seville Bio for paraffin sectioning. After dehydration, the sections were sequentially placed in xylene I for 10 min, xylene II for 10 min, absolute ethanol I for 5 min, absolute ethanol II for 5 min, and 95 %, 90

%, 80 %, and 70 % alcohol for 5 min each. Finally, the sections were rinsed in distilled water. The sections were then stained with hematoxylin for 10 min and eosin staining solution for 1-3 min. After mounting in neutral gum, the sections were observed and photographed using a microscope (Nikon).

Western blotting

Cell populations induced for 10 days with different concentrations of Vitamin B6 were collected and lysed using RIPA buffer (Solarbio, R0010) to extract proteins. The protein concentration was determined, and 20 μg of total cellular protein was mixed with 5 μL of sample buffer and boiled for 3-5 minutes to denature the protein. The protein was then separated by a precast gel (Vazyme, E304-01) from 12% Sure PAGETM, transferred to nitrocellulose membranes, semi-dried, and blocked with 5% skimmed milk at room temperature for 2 hours. Primary antibodies against H3K4me2 (0.2825 μg/ml, Abcam, ab32356) and H3 (0.5μg/ml, Abcam, ab1791) were added to the membranes, which were incubated over-night at 4°C. After washing with PBST, Goat Anti-Rabbit IgG H&L (HRP) (0.4 μg /ml, Abcam, ab6721) was added and incubated at 37°C for 2 hours. The membranes were then imaged and photographed using an imager (BIO-RAD, 733BR2897).

Data analysis

qRT-PCR, luciferase reporter assay, FC, and IF were each repeated three times. Data analysis was performed using Student's t-test with the SPSS 26.0 software package. Graphs were created using GraphPad Prism 6. The principle of randomization was followed throughout the experiment. All data are presented as mean ± standard error (X ± SEM).

Results

miR-1458 presents dynamic changes during the formation of SSCs

To identify key miRNAs, we established an in vitro SSCs induction model (Fig. 1A). We collected ESCs (c_0), self-differentiated cells at 4 days (z_4) and 10 days (z_10), and RA-induced cells at 4 days (R_4) and 10 days (R_10) for transcriptome sequencing. We identified a total of 671 miRNAs (Table S1), out of which 101 miRNAs were significantly

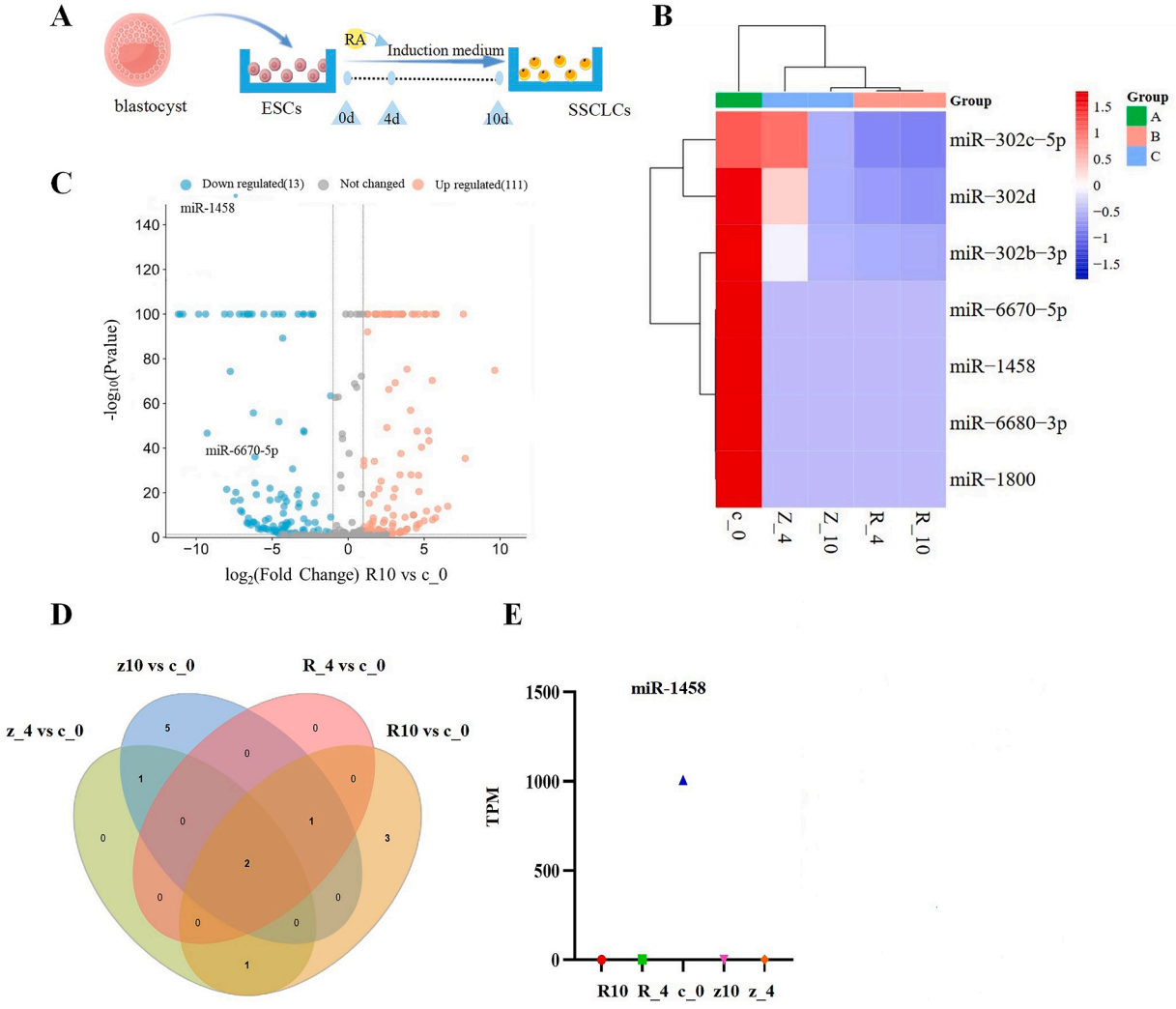

Fig. 1. miR-1458 affects the production of spermatogonial stem cells. (A)Schematic diagram of induced SSCs. (B)The expression profiles of seven miRNAs were analyzed in five different comparisons using miRNA microarray with |log2(fold change)|>8. Hierarchical clustering was performed to visualize the similarity of miRNA expression patterns. The colors used in the visualization indicate increased expression (red) and decreased expression (green) relative to the mean expression levels. (C)Three-point clustering visualization of miRNA expression patterns by three-point clustering of 7 miRNAs screened by miRNA microarray with |log2(fold change)|>8. (D)Venn analysis of differentially expressed miRNAs in five comparisons. (E)Taking the expression level of miRNAs in c_0 as a control, and limited by |log2(fold change)|>8, miR-1458 was expressed in ESCs (c_0), self-differentiation 4d (z-4), self-differentiation 10d (z10), TPM values in RA induction 4d (R4), RA induction 10d (R10).

upregulated and 105 miRNAs were significantly downregulated ($P < 0.01$) during the transition from ESCs to SSCs (Tables S2 and S3). To determine the key miRNAs in SSCs development, we focused on |log2 (fold change)|>8 differential miRNAs and performed cluster analysis on them (Fig. 1B). The volcano plot results showed that miR-1458 had the most significant difference in the formation of RA-induced SSCs (Fig. 1C). We performed Wayne analysis on the differential miRNAs, revealing two differentially expressed miRNAs during the differentiation of ESCs to SSCs, namely miR-1458 and miR-6670-5p (Fig. 1D). The RNA-seq results revealed that miR-1458 expression was exclusive to ESCs (Fig. 1E and Table S4), our previous quantitative results are consistent with the sequencing data (Geng et al., 2023). In addition, we have previously demonstrated that the target genes of miR-1458 are associated with (Geng et al., 2023) . Based on these observations, we further investigated the role of miR-1458 in SSCs development.

Inhibiting the expression of miR-1458 promotes the formation of SSCs

In order to confirm the hypothesis that miR-1458 plays a crucial role in SSCs formation, we utilized the previously established in vitro induction model of embryonic stem cells (ESCs) to differentiate into SSCs using RA. We successfully transfected miR-1458 mimics and inhibitor and conducted morphological observations. The results showed that transfection with miR-1458 inhibitor in the presence of RA resulted in a higher number of embryoid bodies (EBs) on day six and an increased number of Spermatogonial stem cell-like cells (SSCLCs) on day ten. In contrast, miR-1458 mimics delayed the emergence of EBs until day four of culture and showed fewer SSCLCs on day ten (Fig. 2A). Gene expression analysis demonstrated that interfering with the expression of miR-1458 resulted in significantly up-regulated expression levels of the germ cell marker gene *Cvh* and the SSCs marker gene *integrin β1* compared to the normal RA induction process ($P < 0.05$) (Fig. 2B). Conversely, overexpressing miR-1458 presented utterly opposite results. IF and flow FC showed that inhibiting the expression of miR-1458 promoted the formation of SSCs ($P < 0.01$) (Fig. 2C and D). In order to further elucidate the role of miR-1458 in the formation of SSCs, we injected miR-1458 inhibitor and miR-1458 mimics into the testes of chicken embryos at 10 days. Then we incubated them until 18.5 days to collect differently treated chicken embryos. Paraffin slices were prepared, and IHC assays using integrin β1 antibody were performed (Fig. 2E). The results showed that the number of SSCs in the testis collected after miR-1458 interference was significantly reduced compared with the average incubation process ($P < 0.01$). All of these results indicate that inhibiting the expression of miR-1458 promotes the formation of SSCs.

TBX6 is a downstream target gene of miR-1458 in the formation of SSCs

In our previous study, we designed mutation sites in the 3′ UTR region of miR-1458 and *TBX6*, demonstrating that miR-1458 mimics can enhance the activity of miR-1458, thereby increasing the transcriptional regulation of *TBX6* (Geng et al., 2023). To further elucidate the biological functions of TBX6, we conducted a PPI analysis. The results indicated that TBX6 exhibits significant interactions and co-expression with proteins such as Fibroblast Growth Factor 8 (FGF8), SOX2, and WNT3A (Fig. 3A and B). GO analysis of TBX6 function indicated significant enrichment in pathways related to Somitogenesis, cell fate commitment, and embryo development (Fig. 3C). Subsequently, we employed a miR-1458 inhibitor and inhibitor NC to further validate the targeting relationship between miR-1458 and TBX6. Dual-luciferase reporter assays showed that, compared to the 3′ UTR-WT + mimics-NC group, co-transfection of 3′ UTR-WT + miR-1458 mimics resulted in a significant decrease in luciferase activity ($P < 0.05$). In contrast, when co-transfecting 3′ UTR-WT with the miR-1458 inhibitor, luciferase activity significantly increased compared to the 3′ UTR-WT + inhibitor-NC group ($P < 0.05$). Additionally, co-transfection of 3′ UTR-MUT + miR-1458 mimics and 3′ UTR-MT + miR-1458 inhibitor showed no significant differences in luciferase activity compared to the 3′ UTR-MUT + mimics-NC and 3′ UTR-MT + inhibitor-NC groups, respectively (Fig. 3D). Therefore, we infer that TBX6, as a downstream target gene of miR-1458, may play a role in the differentiation process from ESCs to SSCs.

TBX6 plays an opposite role to miR-1458 in Spermatogonial stem cell fate determination

To investigate the role of *TBX6* in the formation of SSCs, we generated active overexpression (**OE**) and interference [short hairpin (**SH**)] vectors of *TBX6*, designated as TBX6-OE and TBX6-SH, respectively. These vectors were transfected into ESCs in vitro, and their effects on SSCs formation were evaluated using the RA induction system. Throughout the induction process, observations of cell morphology revealed that embryoid bodies (**EBs**) appeared on day four after RA induction (Fig. 4A), and EBs began to rupture by day eight after RA induction. After transfection with TBX6-SH, the number of EBs that appeared during the induction process was significantly lower than that of control. We then analyzed the mRNA expression levels of germ cell line-age-specific biomarkers upon differentiation induction, including *Cvh* and *integrin β1*. The depletion of *TBX6* expression was accompanied by a significant decrease in the genes mentioned above ($P < 0.01$) (Fig. 4B). To elucidate the effect of *TBX6* on the formation of SSCs, cells after 10 days of induction were collected and analyzed by IF and FC (Fig. 4C and D). The results demonstrate that the number of integrin β1+ cells significantly decreased after *TBX6* interference compared with routine RA induction ($P < 0.01$).

To further understand the function of *TBX6* during the formation of SSCs, TBX6-OE, and TBX6-SH were injected into the testis of chicken embryos (10 days) and incubated until 18.5 days for IHC using an integrin β1 antibody. The analysis showed that the number of integrin β1+ cells in the testis significantly increased after *TBX6* overexpression compared with the control group ($P < 0.05$) (Fig. 4E). In summary, this study suggests that the downstream target gene *TBX6* of miR-1458 can promote the formation of SSCs both in vivo and in vitro.

Screening of differential metabolites during SSCs formation

Cellular energy metabolites can act as upstream miRNA regulators and participate in miRNA's transcriptional regulation. On the other hand, miRNA can regulate the expression of metabolic enzymes and regulate cellular energy metabolism (Jin and Wei, 2014). In order to screen differential metabolites, this study utilized PCA to analyze the sequencing data, reflecting the variability between sample groups and within groups at the overall level. By observing the PCA statistical analysis results between the ESCs Male and SSCs groups, significant differences were observed between the two cells (Fig. 5A). Then, we performed correlation analysis on the sequencing data and found that the Pearson coefficients between the ESCs Male group and SSCs were more outstanding than 0.95 (Fig. 5B). Next, we performed cluster analysis on the sequencing data and found that Vitamin B6 has different expression patterns in ESCs and SSCs (Fig. 5C). After analyzing the functions and effects of these metabolites on metabolic pathways, we detected the concentration of Vitamin B6 in ESCs and SSCs. The results showed that the expression level of Vitamin B6 in ESCs was significantly higher than that in SSCs ($P < 0.01$) (Fig. 5D). Therefore, Vitamin B6 was identified as a critical candidate metabolite for further investigation.

Vitamin B6 suppressed the lineage specification of SSCLCs

To investigate the effect of vitamin B6 on the fate of SSCs, different concentrations of vitamin B6 were added in vitro to determine the formation efficiency of SSCs using the RA-induced differentiation model. To eliminate the potential effect of cell proliferation on the formation

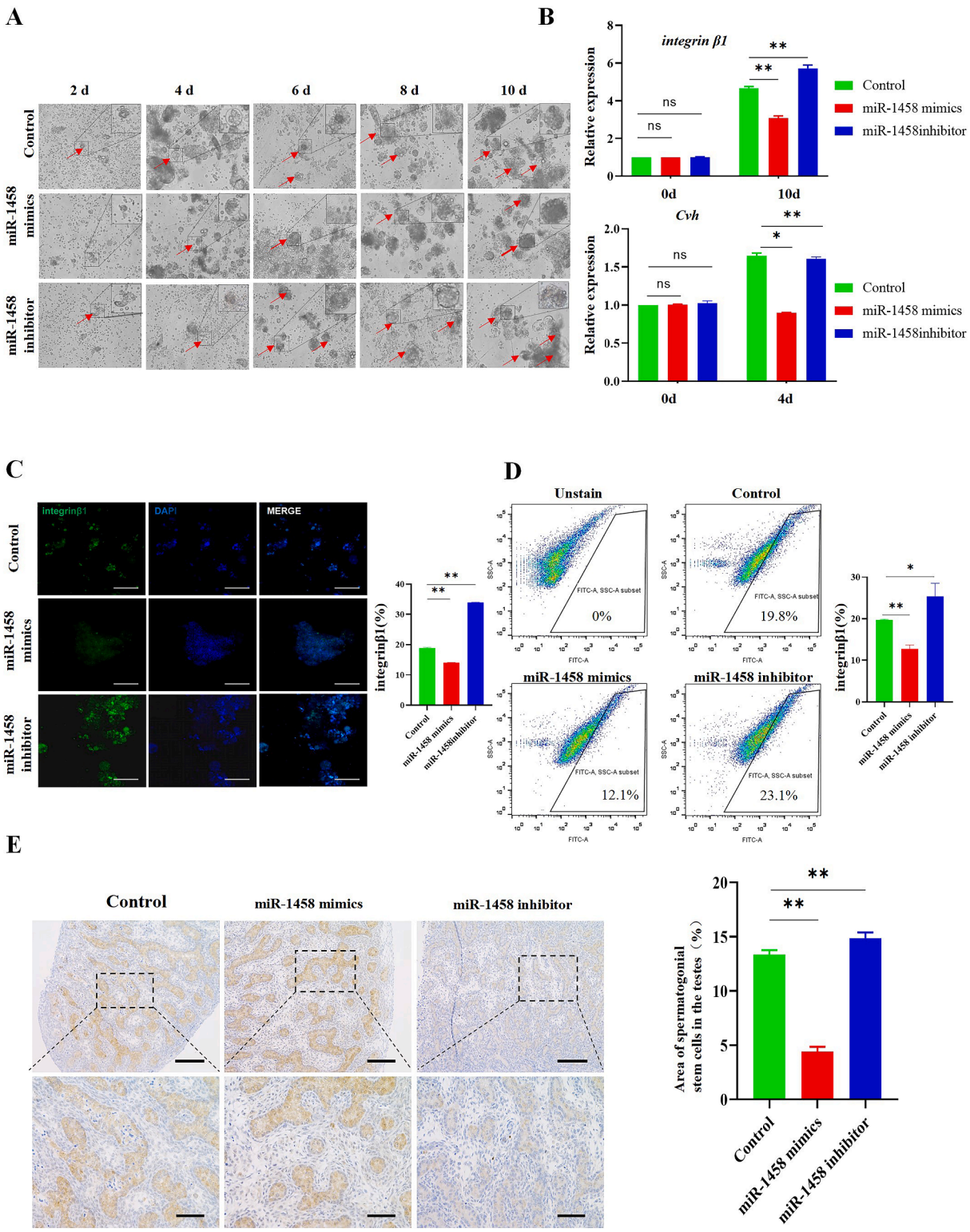

Fig. 2. miR-1458 regulates spermatogonia stem cell generation. (A) Morphological observation of embryoid number in vitro induction model of SSCs following miR-1458 significant upregulation and interference. RA induction served as a control. Scale bar: 60 μm (n = 3 independent experiments). (B) Expression of the reproductive marker gene (*Cvh*) and SSCs marker gene *(integrin β1)* in SSCLC was detected by qRT-PCR after significant upregulation and interference of miR-1458 in vitro (data shown as mean ± SEM, n = 3 independent experiments, $^{*}P < 0.05$, $^{**}P < 0.01$, ns, not significant, one-way ANOVA). (C) The efficiency of SSCs differentiation was tested by IF using integrin β1 antibody at 10 days post-induction. Scale bar: 200 μm (n = 3 independent experiments). (D) SSCs formation efficiency following miR-1458 significant upregulation or interference was tested in vitro and assessed by flow cytometry using integrin β1 antibody (data shown as mean ± SEM, n = 3 independent experiments, $^{*}P < 0.05$, $^{**}P < 0.01$, ns, not significant, one-way ANOVA). (E) The results of HE examination using integrin β1 showed that interference of miR-1458 increased SSCs number in the testis, while significant upregulation of miR-1458 decreased SSCs number in the testis. The segmentation module of the Image J software counted the number of SSCs. Scale bars: 200 μm (upper row), 40 μm (lower row) (data shown as mean ± SEM, n = 3 independent experiments, $^{*}P < 0.05$, $^{**}P < 0.01$, ns, not significant, one-way ANOVA).

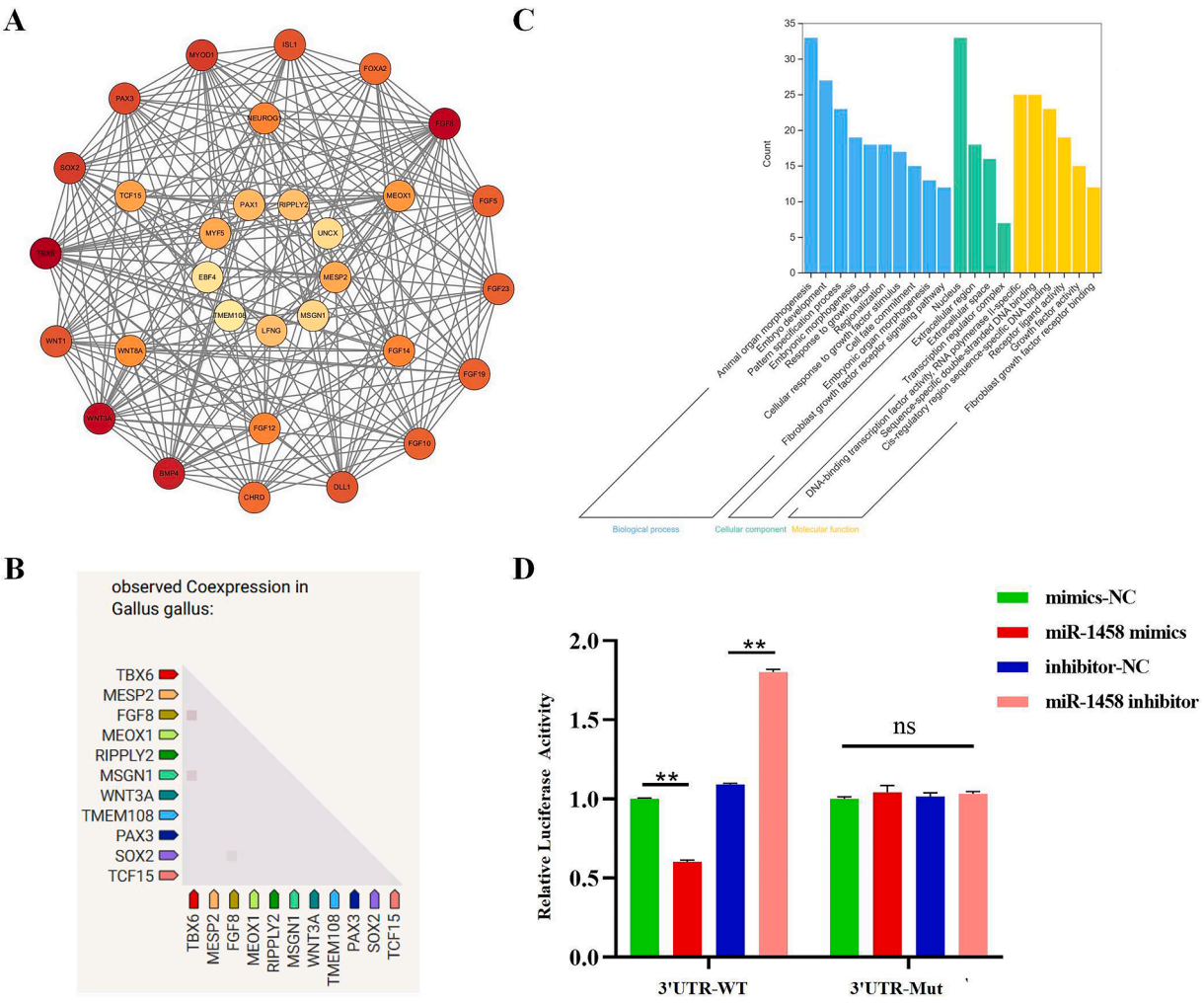

Fig. 3. TBX6 is a Target Gene of miR-1458. (A) Protein-protein interaction analysis of TBX6. (B) Co-expression of TBX6 with interacting proteins. (C) GO functional enrichment analysis of TBX6 interacting proteins. (D) Relative luciferase expression of TBX6 after co-transfection with miR-1458 mimics, mimics-NC, miR-1458 inhibitor, and inhibitor-NC in chicken DF-1 cells. (Data shown as mean ± SEM, n = 3 independent experiments, $^{*}P < 0.05$, $^{**}P < 0.01$, ns, not significant, one-way ANOVA).

efficiency of SSCLCs when adding Vitamin B6, the concentration of Vitamin B6 that does not affect the proliferation of ESCs was screened through EDU and JC-1 assays, and the optimal concentration of Vitamin B6 was determined to be 20 μM (Fig. S1A–C). Following the addition of Vitamin B6, cell morphology observation showed that the number of EBs throughout the process was significantly lower than that of the control group (Fig. 6A). Additionally, the key SSCs regulators *Cvh* and *integrinβ1* were significantly reduced in the Vitamin B6 group ($P < 0.01$) (Fig. 6B). IF and FC analyses also showed similar results (Fig. 6B and C). Compared with normal RA induction, the number of integrin β1+ cells were significantly decreased after adding Vitamin B6 ($P < 0.01$) (Fig. 6C and D).

We next investigated whether there is a regulatory relationship between Vitamin B6 and miR-1458. By adding Vitamin B6 to the RA induction medium, we found that the expression of miR-1458 in the Vitamin B6 group was significantly higher than that in the control group ($P < 0.01$) (Fig. 6E). A dual luciferase reporter assay showed that compared with pGL3-basic, the luciferase activity of Basic-miR-1458 was significantly up-regulated ($P < 0.01$). Compared to transfecting Basic-miR-1458 alone, co transfection with Vitamin B6 resulted in a significant increase in dual luciferase activity ($P < 0.01$) (Fig. 6F). In order to investigate whether Vitamin B6 is involved in intracellular epigenetic modification, we detected the level of histone H3K4me2 at different concentrations of Vitamin B6 using Western blot analysis. The results showed that the level of histone H3K4me2 varied under different concentrations of Vitamin B6, indicating that Vitamin B6 can participate in the methylation modification of histone H3K4me2 in cells (Fig. 6G). Therefore, we preliminarily verified that Vitamin B6 can regulate the expression of miR-1458 by changing the epigenetic modification of the miR-1458 promoter region, thereby affecting the formation efficiency of SSCs.

Discussion

The formation of SSCs is regulated by a complex network of various factors, with miRNAs playing a significant role in their development (Wang et al., 2019; Xu et al., 2020; Chen et al., 2022). Multiple studies have shown that miRNAs are crucial regulators in the proliferation, differentiation, individual development, and maintenance of homeostasis in almost all cell types (McIver et al., 2012; Luo et al., 2015; Noveski et al., 2016; Tuysuz et al., 2021; Nazri et al., 2023). Therefore, we hypothesize that there may also be key miRNAs involved in the formation of SSCs. By comparing the expression of miRNAs during the developmental stages of ESCs and SSCs, we identified seven differentially expressed miRNAs. Thus, we infer that miRNAs may have potential functions in the formation of germ cells, a finding consistent with existing literature (McDonnell et al., 2016). Additionally, we have previously demonstrated that the expression level of miR-1458 significantly

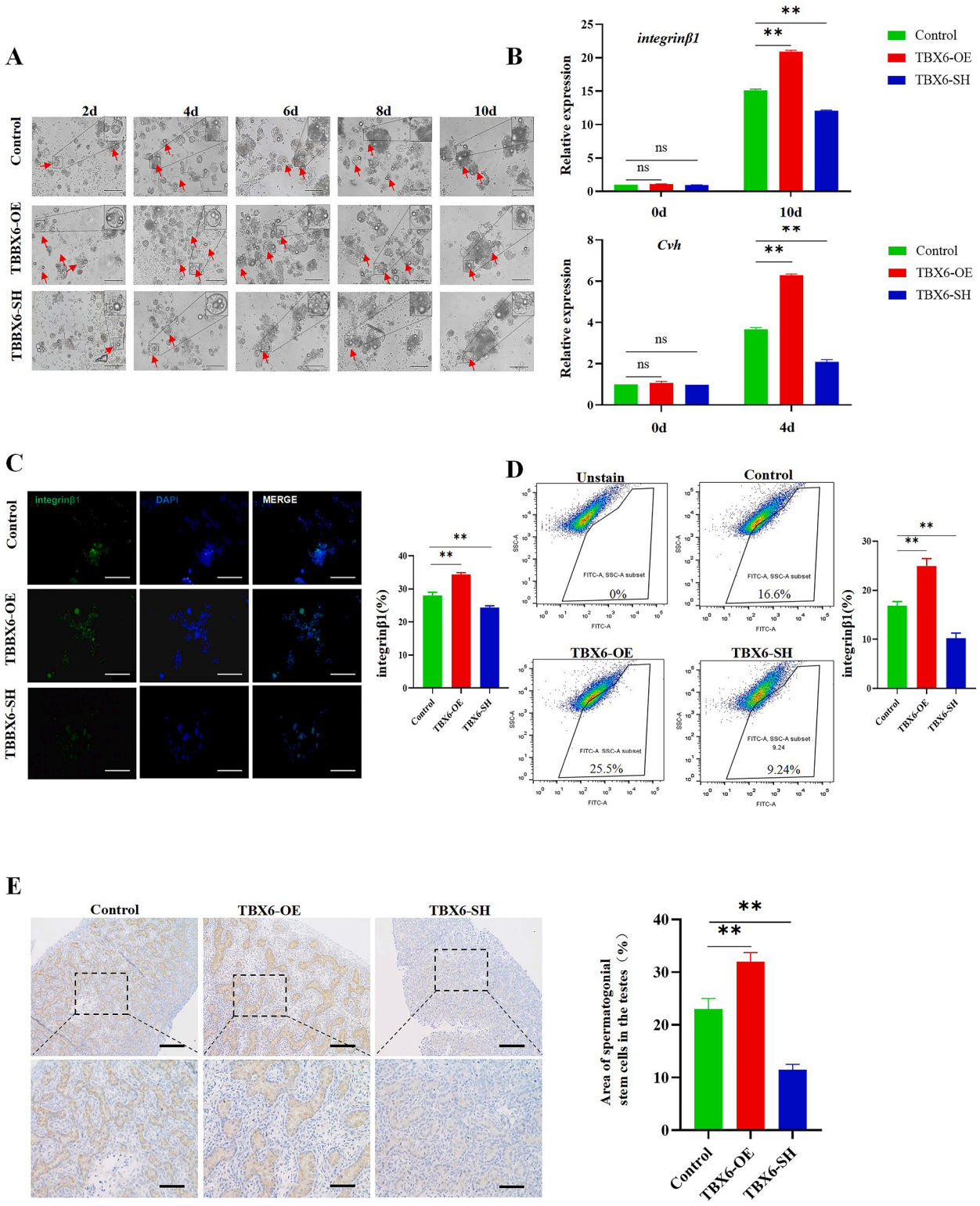

Fig. 4. TBX6 promotes fate determination in Spermatogonial stem cells. (A) Morphological observation of embryoid number in an in vitro SSCs induction model following *TBX6* overexpression and interference; TBX6-OE indicates overexpression of TBX6; TBX6-SH indicates interference of TBX6; RA induction served as a control. Scale bar: 200 μm (n = 3 independent experiments). (B) Expression of the reproductive marker gene (*Cvh*) and SSCs marker gene (*integrin β1*) in SSCLC was detected by qRT-PCR after overexpression and interference with TBX6 in vitro (data shown as mean ± SEM, n = 3 independent experiments, $^{*}P < 0.05$, $^{**}P < 0.01$, ns, not significant, one-way ANOVA). (C) The efficiency of SSCs differentiation was tested by IF using integrin β1 antibody at 10 days post-induction. Scale bar: 200 μm (n = 3 independent experiments). (D) SSCs formation efficiency following TBX6 overexpression or interference was tested in vitro and assessed by flow cytometry using integrin β1 antibody (data shown as mean ± SEM, n = 3 independent experiments, $^{*}P < 0.05$, $^{**}P < 0.01$, ns, not significant, one-way ANOVA). (E) The results of IHC using integrin β1 antibody showed that interference with TBX6 increased SSCs numbers in testes, whereas overexpression of TBX6 decreased SSCs numbers in testes. The segmentation module of the Image J software counted the number of SSCs. Scale bars: 200 μm (upper row), 40 μm (lower row) (data shown as mean ± SEM, n = 3 independent experiments, $^{*}P < 0.05$, $^{**}P < 0.01$, ns, not significant, one-way ANOVA).

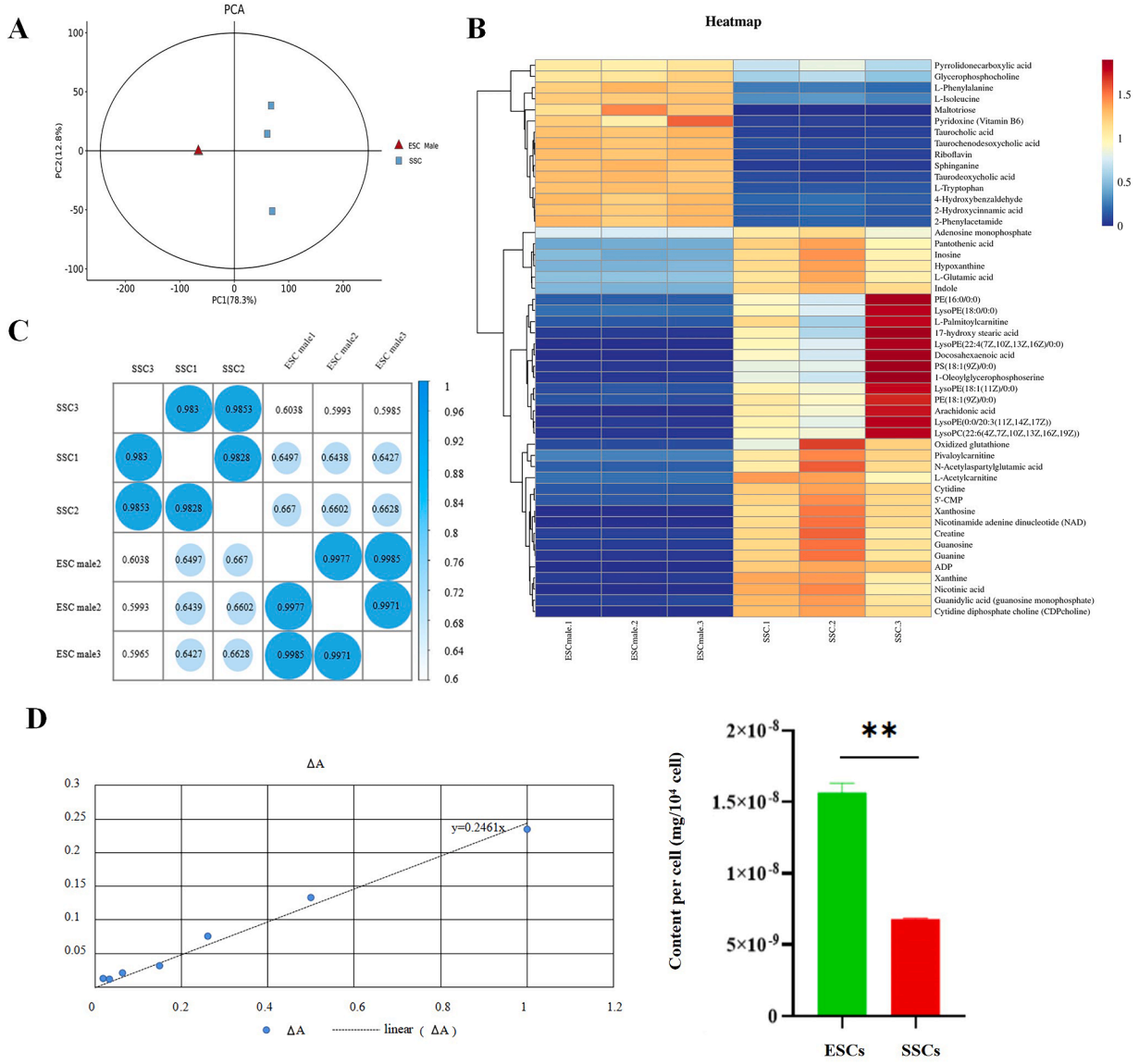

Fig. 5. Screening of Vitamin B6, a differential metabolite, during the formation of SSCs. (A) Unsupervised principal component analysis (PCA) of ESCs male and SSCs with six biological replicates. (B) Pearson correlation coefficient analysis of differential metabolites in ESCs male and SSCs. (C) Heatmap reveals metabolite expression patterns in ESCs and SSCs. Metabolites with P-values for differential metabolites in the first 80 samples were analyzed. Red corresponds to upregulation; Blue corresponds to downregulation. (D) Analysis of Vitamin B6 concentrations in ESCs and SSCs (data shown as mean ± SEM, n = 3 independent experiments, $*P < 0.05$, $**P < 0.01$, ns, not significant, one-way ANOVA).

decreases during the differentiation process from ESCs to SSCs, with its downstream target genes enriched in pathways related to germ cell differentiation, such as the TGF-beta signaling pathway (Geng et al., 2023). Through the transfection of miR-1458 mimics and inhibitors, we found that the inhibition of miR-1458 expression promotes the formation of SSCs. This result further supports Cutting's assertion regarding the role of miR-1458 in the differentiation of ESCs (Cutting et al., 2012). However, the upstream regulatory mechanisms of miR-1458 and its role in regulating the lineage specification of SSCs remain to be further investigated.

An important finding of this study is that *TBX6*, as a downstream target gene of miR-1458, is associated with the lineage specification of SSCs, further expanding our previous research on the regulation of *TBX6* by miR-1458 (Geng et al., 2023). Existing literature indicates that *TBX6*, a T-box transcription factor, is primarily enriched in the paraxial/prechordal mesoderm and is closely related to somatic cell formation (Nohe et al., 2004; Sadahiro et al., 2018). Although the role of *TBX6* in somatic development is well recognized, its functions in other mesodermal or germ cells remain unclear. Notably, Yakhkeshi et al. (2018) demonstrated that *TBX6* can directly induce the differentiation of fibroblasts and pluripotent stem cells from mice and humans into cardiac mesodermal cells upon injection. Additionally, Chapman (2019) found that reduced expression levels of Tbx6 lead to impaired intermediate formation in mouse embryos. This finding suggests that *TBX6* not only plays a crucial role in somatic cell formation but may also be involved in the differentiation process. In our experiments, we observed that *TBX6*, as a downstream target gene of miR-1458, promotes the lineage specification of SSCs. This indicates that, although the mechanisms of *TBX6* function in germ cells are not fully understood, it similarly plays an important role in regulating the differentiation of SSCs. Furthermore, combining our functional validation results for miR-1458, we found that TBX6′s role contradicts that of miR-1458, as it is targeted and regulated by miR-1458 in the context of SSC fate. Our results provide further evidence of the significant role of *TBX6* in cell differentiation, consistent with previous studies.

The process by which cells transition from pluripotency to terminally

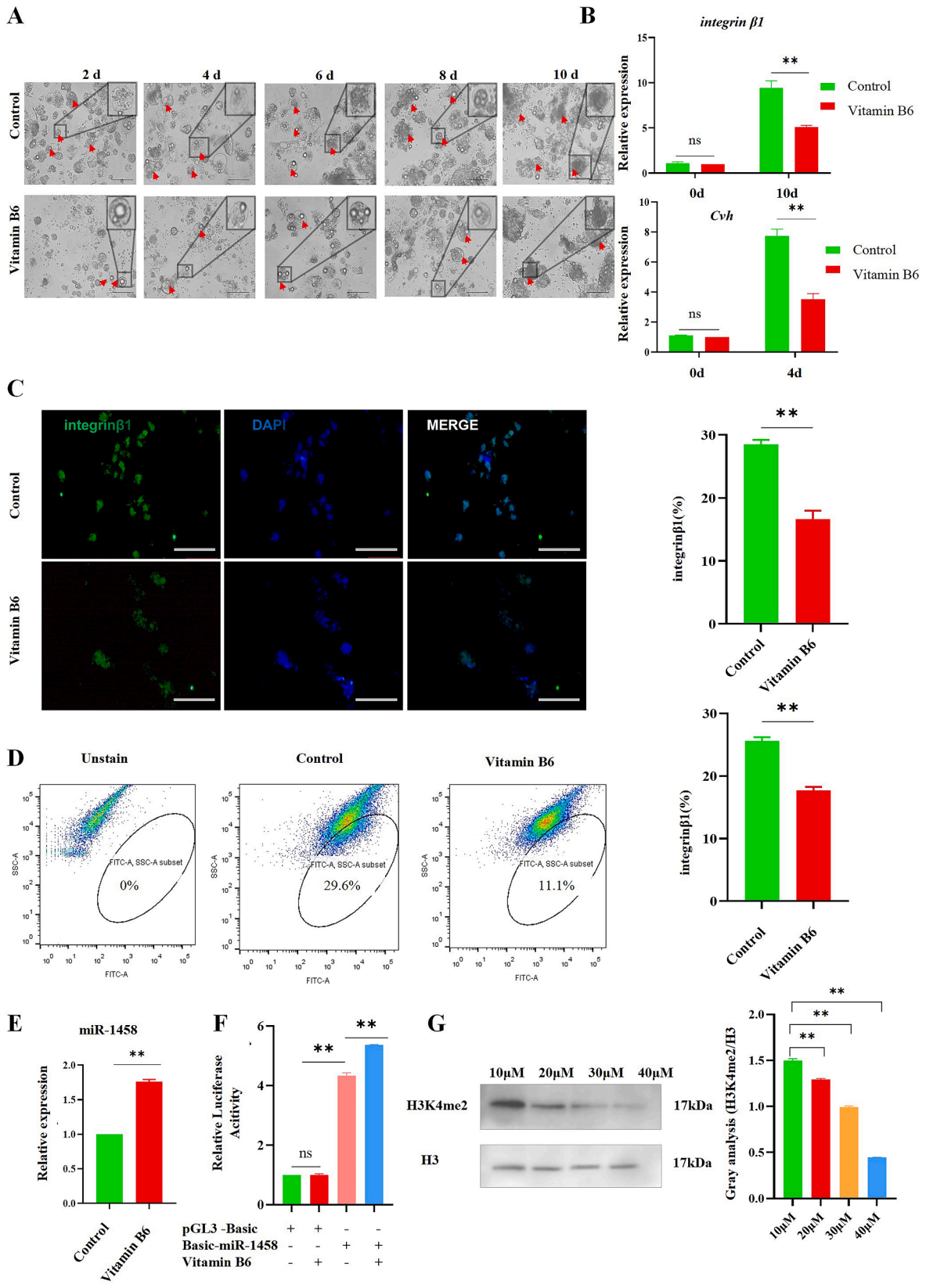

(caption on next page)

Fig. 6. Vitamin B6 inhibits the lineage specification of SSCLCs. (A) Morphological observation of embryoid number in vitro induction model of SSCs after addition of 20 μM Vitamin B6 in vitro. RA induction served as a control. Scale bar: 60 μm (n = 3 independent experiments). (B) Expression of reproductive marker gene (*Cvh*) and SSCs marker gene (*integrin β1*) in SSCLC was detected by qRT-PCR after addition of 20 μM Vitamin B6 in vitro (data shown as mean ± SEM, n = 3 independent experiments, $^{*}P < 0.05$, $^{**}P < 0.01$, ns, not significant, one-way ANOVA). (C) The efficiency of SSCs formation supplemented with 20 μM Vitamin B6 was tested by IF using integrin β1 anti-body on day ten post-induction. Scale bar: 200 μm (n = 3 independent experiments). (D) SSCs formation efficiency was tested in vitro after the addition of 20 μM Vitamin B6 as assessed by flow cytometry using integrin β1 antibody (data shown as mean ± SEM, n = 3 independent experiments, $^{*}P < 0.05$, $^{**}P < 0.01$, ns, not significant, one-way ANOVA). (E) miR-1458 expression in SSCLCs was detected by qRT-PCR after in vitro addition of 20 μM Vitamin B6 (data shown as mean ± SEM, n = 3 independent experiments, $^{*}P < 0.05$, $^{**}P < 0.01$, ns, not significant, one-way ANOVA). (F) Relative luciferase expression in the promoter region of miR-1458 after transfection with PGL3-basic vector, 20μM Vitamin B6 co-transfected with PGL3-basic vector, Basic-miR-1458 vector and 20μM Vitamin B6 co-transfected with Basic-miR-1458 in vitro, respectively. (Data shown as mean ± SEM, n = 3 independent experiments, $^{*}P < 0.05$, $^{**}P < 0.01$, ns, not significant, one-way ANOVA). (G) H3K4me2 levels in SSCLCs supplemented with differ-ent concentrations of Vitamin B6 in vitro (left). ImageJ software was used for gray-level analysis (right) (Data shown as mean ± SEM, n = 3 independent experiments, $^{*}P < 0.05$, $^{**}P < 0.01$, one-way ANOVA).

differentiated cells with distinct functions is accompanied by changes in metabolic patterns and the epigenetic landscape (Kinnaird et al., 2016; D'Aniello et al., 2019; Moreno-Yruela et al., 2022). Previous studies have shown that intracellular metabolites can directly participate in the epigenetic dynamics regulating gene expression by providing specific metabolic pathways that produce enzymes, cofactors, or substrates, thereby facilitating or amplifying the differentiation signals of pluripotent stem cells (Moussaieff et al., 2015; Chantranupong et al., 2015; Reid et al., 2017). Stegen et al. (2022) found that glutamine regulates the expression of chondrogenic genes through histone acetylation mediated by glutamate dehydrogenase, promoting the formation of chondrocytes. Similarly, Sim et al. (2022) demonstrated that methionine deficiency leads to a reduction in intracellular S-adenosylmethionine (**SAM**), triggering the transition of pluripotent stem cells (**PSC**s) to a differentiated state. Thus, we hypothesize that certain metabolites may act as upstream regulatory factors of miR-1458, participating in the regulation of SSC lineage specification. Our results reveal that Vitamin B6 is expressed at significantly higher levels in ESCs compared to SSCs, and that low levels of Vitamin B6 specifically promote the formation of SSCs, underscoring its important role in regulating the germ lineage. Fayomi and Orwig (2018) also demonstrated that elevated levels of Vitamin B6 in mice delay spermatogenesis, reduce sperm counts, and impair sperm motility, which is consistent with our findings. Notably, we observed that low levels of Vitamin B6 can suppress intracellular miR-1458 expression, contradicting the functional validation results for miR-1458. Therefore, we speculate that low levels of Vitamin B6 may influence SSCs fate determination as an upstream regulatory factor of miR-1458.

Histone modification, as one of the important regulatory mechanisms in epigenetics, alters chromatin structure and regulates gene expression through at least eight modification methods, including histone methylation, acetylation, phosphorylation, and ubiquitination (Tyurin-Kuzmin et al., 2020). Zuo et al. (2021) found that the demethylation of H3K4me3 to H3K4me2 affects the development of germ cells. Vitamin B6 has been shown to influence the differentiation of pluripotent cells. Its mechanism of action involves providing methyl donors in one-carbon metabolism, participating in DNA and histone methylation, and thereby regulating the pluripotent state of cells (Tischler et al., 2019). In this study, we demonstrate that low levels of Vitamin B6 can reduce the level of H3K4me2 modification in chicken germ cells, thereby inhibiting the transcription of miR-1458 and participating in the formation of SSCs. We identify Vitamin B6 as an upstream regulatory factor involved in the transcriptional process of miR-1458, further expanding the significance of metabolites and their mediating epigenetic modifications in the lineage specification of germ cells.

In conclusion, this study demonstrates that low levels of Vitamin B6 inhibit the transcriptional activity of miR-1458 by reducing intracellular H3K4me2 levels, thereby increasing the expression of the downstream target gene *TBX6* and ultimately promoting the formation of SSCs. We have constructed a regulatory network involving Vitamin B6- H3K4me2- miR-1458- TBX6 in the process of SSCs formation, revealing how key miRNAs serve as a bridge between epigenetic modifications and cell fate determination. However, it is essential to note that most of the miRNA-related germline findings were obtained through in vitro studies. Therefore, in vivo, studies are needed to validate these findings and potentially translate them into clinical applications.

Conclusions

Low levels of the cellular metabolite Vitamin B6 can inhibit H3K4me2 in the miR-1458 promoter region, thereby suppressing the transcription of miR-1458, which leads to increased expression of its downstream target gene *TBX6* and promotes the formation of SSCs.

Financial support statement

This work was financially supported by funding from National Natural Science Foundation of China, Grant No. 32272857, National Key R&D Program of China, Grant No. 2021YFD1200305. The content is solely the responsibility of the authors and does not necessarily represent the official views of any of the funding agencies.

CRediT authorship contribution statement

Qingqing Geng: Conceptualization, Investigation, Writing – original draft. **Cai Hu:** Resources. **Ziduo Zhao:** Software, Formal analysis. **Zhe Wang:** Formal analysis, Visualization. **Fufu Cheng:** Software. **Jing Chen:** Methodology. **Qisheng Zuo:** Project administration, Supervision, Validation. **Yani Zhang:** Conceptualization, Funding acquisition, Writing – review & editing.

Declaration of competing interest

The authors declare no competing interests.

Supplementary materials

Supplementary material associated with this article can be found, in the online version, at doi:10.1016/j.psj.2024.104583.

Data availability

Data is contained within the article or Supplementary Material. The dataset generated and/or analysed during the current study is available in the NCBI repository. The data can be accessed by BioProject submission: PRJNA1149557.

References

Airaksinen, M.S., Saarma, M., 2002. The GDNF family: signalling, biological functions and therapeutic value. Nat. Rev. Neurosci. 3, 383–394.

Boellaard, W.P.A., Stoop, H., Gillis, A.J.M., Oosterhuis, J.W., Looijenga, L.H.J., 2017. VASA mRNA (DDX4) detection is more specific than immunohistochemistry using poly- or monoclonal antibodies for germ cells in the male urogenital tract. Med. (Baltim.) 96, e7489.

Chantranupong, L., Wolfson, R.L., Sabatini, D.M., 2015. Nutrient-sensing mechanisms across evolution. Cell 161, 67–83.

Chapman, D.L., 2019. Impaired intermediate formation in mouse embryos expressing reduced levels of Tbx6. Genesis 57, e23270.
Chen, W., Cui, Y., Ning, M., Zhang, H., Yin, C., He, Z., 2022. The mechanisms and functions of microRNAs in mediating the fate determinations of human spermatogonial stem cells and Sertoli cells. Semin. Cell Dev. Biol. 121, 32–39.
Chen, H.-H., Welling, M., Bloch, D.B., Muñoz, J., Mientjes, E., Chen, X., Tramp, C., Wu, J., Yabuuchi, A., Chou, Y.-F., Buecker, C., Krainer, A., Willemsen, R., Heck, A.J., Geijsen, N., 2014. DAZL limits pluripotency, differentiation, and apoptosis in developing primordial germ cells. Stem Cell Rep. 3, 892–904.
Clotaire, D.Z.J., Du, X., Wei, Y., Yang, D., Hua, J., 2018. miR-19b-3p integrates Jak-Stat signaling pathway through Plzf to regulate self-renewal in dairy goat male germline stem cells. Int. J. Biochem. Cell Biol. 105, 104–114.
Cutting, A.D., Bannister, S.C., Doran, T.J., Sinclair, A.H., Tizard, M.V.L., Smith, C.A., 2012. The potential role of microRNAs in regulating gonadal sex differentiation in the chicken embryo. Chromos. Res. 20, 201–213.
D'Aniello, C., Cermola, F., Patriarca, E.J., Minchiotti, G., 2019. Metabolic-epigenetic axis in pluripotent State transitions. Epigenomes 3, 13.
Diao, L., Turek, P.J., John, C.M., Fang, F., Reijo Pera, R.A., 2022. Roles of spermatogonial stem cells in spermatogenesis and fertility restoration. Front. Endocrinol. (Lausanne) 13, 895528.
Endo, T., Romer, K.A., Anderson, E.L., Baltus, A.E., de Rooij, D.G., Page, D.C., 2015. Periodic retinoic acid-STRA8 signaling intersects with periodic germ-cell competencies to regulate spermatogenesis. Proc. Natl. Acad. Sci. U.S.A. 112, E2347–E2356.
Fayomi, A.P., Orwig, K.E., 2018. Spermatogonial stem cells and spermatogenesis in mice, monkeys and men. Stem Cell Res. 29, 207–214.
Geng, Q., Cheng, F., Hu, C., Wu, R., Wu, Y., Zhao, Z., Zhao, Z., Zhang, Y., 2023. Verification of the targeting relationship between Rugao Yellow chicken miR-1458 and TBX6. Zhongguo Jiaqin 45, 31–37.
Hickford, D.E., Frankenberg, S., Pask, A.J., Shaw, G., Renfree, M.B., 2011. DDX4 (VASA) is conserved in germ cell development in marsupials and monotremes. Biol. Reprod. 85, 733–743.
Jin, L.-H., Wei, C., 2014. Role of microRNAs in the Warburg effect and mitochondrial metabolism in cancer. Asian Pac. J. Cancer Prev. 15, 7015–7019.
Kinnaird, A., Zhao, S., Wellen, K.E., Michelakis, E.D., 2016. Metabolic control of epigenetics in cancer. Nat. Rev. Cancer 16, 694–707.
Kubota, H., Brinster, R.L., 2018. Spermatogonial stem cells. Biol. Reprod. 99, 52–74.
Li, D., Cheng, S., Zhang, W., Wang, M., Sun, C., Zhang, C., Wang, Y., Jin, J., Zhang, Y., Li, B., 2017. Hedgehog-Gli1 signaling regelates differentiation of chicken (Gallus gallus) embryonic stem cells to male germ cells. Anim. Reprod. Sci. 182, 9–20.
Li, H., Liang, Z., Yang, J., Wang, D., Wang, H., Zhu, M., Geng, B., Xu, E.Y., 2019. DAZL is a master translational regulator of murine spermatogenesis. Natl. Sci. Rev. 6, 455–468.
Luo, Z., Liu, Y., Chen, L., Ellis, M., Li, M., Wang, J., Zhang, Y., Fu, P., Wang, K., Li, X., Wang, L., 2015. microRNA profiling in three main stages during porcine spermatogenesis. J. Assist. Reprod. Genet. 32, 451–460.
McDonnell, E., Crown, S.B., Fox, D.B., Kitir, B., Ilkayeva, O.R., Olsen, C.A., Grimsrud, P. A., Hirschey, M.D., 2016. Lipids reprogram metabolism to become a major carbon source for histone acetylation. Cell Rep. 17, 1463–1472.
McIver, S.C., Stanger, S.J., Santarelli, D.M., Roman, S.D., Nixon, B., McLaughlin, E.A., 2012. A unique combination of male germ cell miRNAs coordinates gonocyte differentiation. PLoS One 7, e35553.
Moreno-Yruela, C., Bæk, M., Monda, F., Olsen, C.A., 2022. Chiral posttranslational modification to lysine ε-amino groups. Acc. Chem. Res. 55, 1456–1466.
Moussaieff, A., Rouleau, M., Kitsberg, D., Cohen, M., Levy, G., Barasch, D., Nemirovski, A., Shen-Orr, S., Laevsky, I., Amit, M., Bomze, D., Elena-Herrmann, B., Scherf, T., Nissim-Rafinia, M., Kempa, S., Itskovitz-Eldor, J., Meshorer, E., Aberdam, D., Nahmias, Y., 2015. Glycolysis-mediated changes in acetyl-CoA and histone acetylation control the early differentiation of embryonic stem cells. Cell Metab. 21, 392–402.
Nazri, H.M., Greaves, E., Quenby, S., Dragovic, R., Tapmeier, T.T., Becker, C.M., 2023. The role of small extracellular vesicle-miRNAs in endometriosis. Hum. Reprod. 38, 2296–2311.
Nohe, A., Keating, E., Knaus, P., Petersen, N.O., 2004. Signal transduction of bone morphogenetic protein receptors. Cell Signal. (Middlet) 16, 291–299.
Noveski, P., Popovska-Jankovic, K., Kubelka-Sabit, K., Filipovski, V., Lazarevski, S., Plaseski, T., Plaseska-Karanfilska, D., 2016. MicroRNA expression profiles in testicular biopsies of patients with impaired spermatogenesis. Andrology 4, 1020–1027.
O'Shea, J.J., Paul, W.E., 2010. Mechanisms underlying lineage commitment and plasticity of helper CD4+ T cells. Science 327, 1098–1102.
Parekh, P.A., Garcia, T.X., Hofmann, M.-C., 2019. Regulation of GDNF expression in Sertoli cells. Reproduction 157, R95–R107.
Reid, M.A., Dai, Z., Locasale, J.W., 2017. The impact of cellular metabolism on chromatin dynamics and epigenetics. Nat. Cell Biol. 19, 1298–1306.
Sadahiro, T., Isomi, M., Muraoka, N., Kojima, H., Haginiwa, S., Kurotsu, S., Tamura, F., Tani, H., Tohyama, S., Fujita, J., Miyoshi, H., Kawamura, Y., Goshima, N., Iwasaki, Y.W., Murano, K., Saito, K., Oda, M., Andersen, P., Kwon, C., Uosaki, H., Nishizono, H., Fukuda, K., Ieda, M., 2018. Tbx6 Induces nascent mesoderm from pluripotent stem cells and temporally controls cardiac versus somite lineage diversification. Cell Stem Cell 23, 382–395 e5.
Samsonova, A., El Hage, K., Desforges, B., Joshi, V., Clément, M.-J., Lambert, G., Henrie, H., Babault, N., Craveur, P., Maroun, R.C., Steiner, E., Bouhss, A., Maucuer, A., Lyabin, D.N., Ovchinnikov, L.P., Hamon, L., Pastré, D., 2021. Lin28, a major translation reprogramming factor, gains access to YB-1-packaged mRNA through its cold-shock domain. Commun. Biol. 4, 359.
Sim, E.Z., Enomoto, T., Shiraki, N., Furuta, N., Kashio, S., Kambe, T., Tsuyama, T., Arakawa, A., Ozawa, H., Yokoyama, M., Miura, M., Kume, S., 2022. Methionine metabolism regulates pluripotent stem cell pluripotency and differentiation through zinc mobilization. Cell Rep. 40, 111120.
Tallquist, M., Kazlauskas, A., 2004. PDGF signaling in cells and mice. Cytokine Grow. Factor Rev. 15, 205–213.
Tischler, J., Gruhn, W.H., Reid, J., Allgeyer, E., Buettner, F., Marr, C., Theis, F., Simons, B.D., Wernisch, L., Surani, M.A., 2019. Metabolic regulation of pluripotency and germ cell fate through α-ketoglutarate. EMBO J. 38, e99518.
Tsogtbaatar, E., Landin, C., Minter-Dykhouse, K., Folmes, C.D.L., 2020. Energy metabolism regulates stem cell pluripotency. Front. Cell Dev. Biol. 8, 87.
Tuysuz, E.C., Ozbey, U., Gulluoglu, S., Kuskucu, A., Sahin, F., Bayrak, O.F., 2021. miRNAs as cell fate determinants of lateral and paraxial mesoderm differentiation from embryonic stem cells. Dev. Biol. 478, 212–221.
Tyurin-Kuzmin, P.A., Molchanov, A.Y., Chechekhin, V.I., Ivanova, A.M., Kulebyakin, K. Y., 2020. Metabolic regulation of mammalian stem cell differentiation. Biochem. (Mosc.) 85, 264–278.
Wang, Y., Bi, Y., Zuo, Q., Zhang, W., Li, D., He, N.-N., Cheng, S., Zhang, Y.-N., Li, B., 2018. MAPK8 regulates chicken male germ cell differentiation through JNK signaling pathway. J. Cell. Biochem. 119, 1548–1557.
Wang, Y., Li, X., Gong, X., Zhao, Y., Wu, J., 2019. MicroRNA-322 regulates self-renewal of mouse spermatogonial stem cells through Rassf8. Int. J. Biol. Sci. 15, 857–869.
Wang, Y., Zuo, Q., Bi, Y., Zhang, W., Jin, J., Zhang, L., Zhang, Y.-N., Li, B., 2017. miR-31 regulates spermatogonial stem cells meiosis via targeting Stra8. J. Cell. Biochem. 118, 4844–4853.
Xian, H., Wang, F., Teng, W., Yang, D., Zhang, M., 2017. Thyroid hormone induce a p53-dependent DNA damage through PI3K/Akt activation in sperm. Gene 615, 1–7.
Xu, C., Shah, M.A., Mipam, T., Wu, S., Yi, C., Luo, H., Yuan, M., Chai, Z., Zhao, W., Cai, X., 2020. Bovid microRNAs involved in the process of spermatogonia differentiation into spermatocytes. Int. J. Biol. Sci. 16, 239–250.
Yakhkeshi, S., Rahimi, S., Sharafi, M., Hassani, S.-N., Taleahmad, S., Shahverdi, A., Baharvand, H., 2018. In vitro improvement of quail primordial germ cell expansion through activation of TGF-beta signaling pathway. J. Cell. Biochem. 119, 4309–4319.
Yang, Q.-E., Racicot, K.E., Kaucher, A.V., Oatley, M.J., Oatley, J.M., 2013. MicroRNAs 221 and 222 regulate the undifferentiated state in mammalian male germ cells. Development 140, 280–290.
Young, J.C., Kerr, G., Micati, D., Nielsen, J.E., Rajpert-De Meyts, E., Abud, H.E., Loveland, K.L., 2020. WNT signalling in the normal human adult testis and in male germ cell neoplasms. Hum. Reprod. 35, 1991–2003.
Zhang, Y., Wang, Y., Zuo, Q., Li, D., Zhang, W., Lian, C., Tang, B., Xiao, T., Wang, M., Wang, K., Li, B., 2016. Effects of the transforming growth factor beta signaling pathway on the differentiation of chicken embryonic stem cells into male germ cells. Cell Reprogram 18, 401–410.
Zhang, Y., Zhang, W., Hu, C., Wang, Y., Wang, M., Zuo, Q., Elsayed, A.K., Li, Y., Li, B., 2021. 2021. miR-302d competitively binding with the lncRNA-341 targets TLE4 in the process of SSC generation. Stem Cell. Int., 5546936
Zuo, Q., Jin, J., Jin, K., Zhou, J., Sun, C., Song, J., Chen, G., Zhang, Y., Li, B., 2020. P53 and H3K4me2 activate N6-methylated LncPGCAT-1 to regulate primordial germ cell formation via MAPK signaling. J. Cell. Physiol. 235, 9895–9909.
Zuo, Q., Jin, K., Wang, M., Zhang, Y., Chen, G., Li, B., 2021. BMP4 activates the Wnt-Lin28A-Blimp1-Wnt pathway to promote primordial germ cell formation via altering H3K4me2. J. Cell. Sci. 134, jcs249375.